

# Edge effects in electrostatic calibrations for the measurement of the Casimir force

Qun Wei<sup>1</sup> and Roberto Onofrio<sup>2,1</sup>

<sup>1</sup>*Department of Physics and Astronomy, Dartmouth College, 6127 Wilder Laboratory, Hanover, NH 03755, USA*

<sup>2</sup>*Dipartimento di Fisica “Galileo Galilei”, Università di Padova, Via Marzolo 8, Padova 35131, Italy*

(Dated: September 8, 2018)

We have performed numerical simulations to evaluate the effect on the capacitance of finite size boundaries realistically present in the parallel plane, sphere-plane, and cylinder-plane geometries. The potential impact of edge effects in assessing the accuracy of the parameters obtained in the electrostatic calibrations of Casimir force experiments is then discussed.

PACS numbers: 12.20.Fv, 03.70.+k, 04.80.Cc, 11.10.Wx

## 1. INTRODUCTION

The Casimir force [1] has been demonstrated in a variety of experimental setups and geometries, yet there is an ongoing reanalysis of the level of accuracy with which it has been determined, which is crucial for assessing reliable limits to the existence of Yukawa forces of gravitational origin predicted by various models [2–4]. In performing Casimir force measurements a crucial role is played by the related electrostatic force calibrations, and mastering all possible systematic effects in the latter is mandatory to assess the precision of the former. The presence of anomalous exponents in the power-law dependence upon distance and the dependence on distance of the minimizing potential [5] have been identified as a possible source of systematic effects, to be carefully scrutinized in each experimental setup [6]. The distance-dependence of the minimizing potential has been recently modeled theoretically, after a first effort reported in [7], in terms of non-equipotential conducting surfaces due to random patterns of patch charges [8]. Here we report results on a further potential source of systematic error by studying, by means of numerical simulations using finite element analysis, the influence of the unavoidable presence of edges on electrostatic calibrations in various geometries (for the influence of edge effects on Casimir forces in peculiar geometries see [9, 10]). We limit the attention to the three geometries that, apart from the crossed-plane investigated in [11], have been extensively discussed for measuring Casimir force so far, *i.e.* the parallel plates [12, 13], the sphere-plane [14–17], and the recently proposed cylinder-plane [18] (see Fig. 1). We discuss the deviations from ideality in all these geometries through the essential knowledge of the capacitance dependence on distance, and its general implications for determining the parameters used in the measurement of the Casimir force. This is performed under the simplifying assumptions that the surfaces are equipotential, *i.e.* by omitting any superimposed effect due to electrostatic patches, and by neglecting the tensorial nature of the capacitance among all the conducting surfaces realistically involved in concrete experimental setups.

## 2. PARALLEL PLATE GEOMETRY

We start our analysis with the parallel plates configuration since this is the simplest geometry even in terms of possible deviations from the ideal, infinite plane case. Moreover, besides having an exact expression in the ideal case of infinite plates, analytical approximate expressions are also available for the capacitance including edge effects [19], allowing to obtain reliable numerical benchmarks. We consider two identical parallel square plates of length  $L$ , and boundary conditions set in such a way that the two plates are at a constant electric potential difference. The total electrostatic potential energy is then computed by numerically solving the Laplace equation using a dedicated finite element analysis software (COMSOL). We evaluate the total electrostatic energy  $W_{\text{el}}$  by summing the electrostatic energy density over a selected volume surrounding the two equipotential surfaces. The capacitance  $C$  can then be calculated from the relationship  $C = 2W_{\text{el}}V^2$ . The parameters of the mesh (mesh size, rate of growth etc.) are carefully chosen and extensively tested to ensure the accuracy of the numerical results. When the distance between the two plates is much smaller than  $L$ , the capacitance obtained from the numerical simulation agrees within 0.01% with the well known analytical formula  $C_{\text{pp}} = \epsilon_0 A/d$ , where  $A$  is the surface area of the plates,  $d$  their separation, and  $\epsilon_0$  the vacuum electric permittivity. However, when the distance becomes larger, the value of the capacitance begins to deviate from the analytical formula. The left plot in Fig. 2 shows the capacitance of two parallel square plates *vs.* distance, together with the expected capacitance for two plates following the infinite surface formula, appearing as a dashed line. The data at large distance deviate significantly from the dashed line, and the fact that they are all above implies that the power-law exponent is softer, *i.e.* in between 0 and -1. This deviation is ascribed to the finite size of the parallel plates. In fact, if only the field lines in the volume delimited by the two plates are used for the sum of the electrostatic energy, which corresponds to ignoring the contribution of the outer region, the capacitance obtained from the nu-

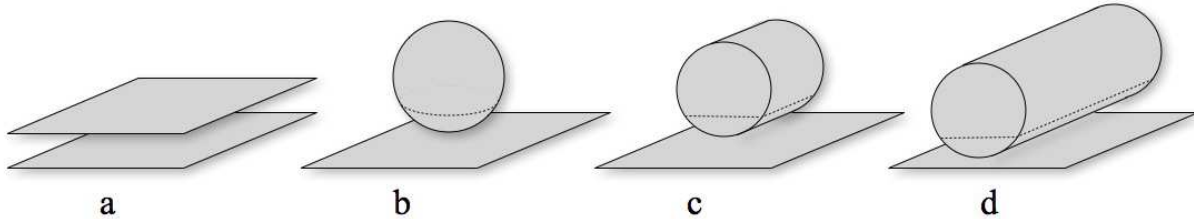


FIG. 1: Selected geometries for the numerical study of finite size effects. Parallel plates of finite size (a); a sphere in front of a finite size plane (b); a cylinder in front of a plane, with width smaller (c) and larger (d) than the size of the plane. In the latter three configurations, a truncated sphere and short and long truncated cylinders, as shown by the dashed lines, have been also studied.

numerical simulation would still agree with the analytical formula even at the largest explored distances. In order to better quantify this deviation we have fitted the capacitance curve by progressively removing points at the largest distance. As shown in the right plot in Fig. 2, the optimal exponent becomes smaller than unity when data at large distance are progressively included in the fit.

### 3. SPHERE-PLANE GEOMETRY

In the case of the sphere-plane geometry, the exact expression for the capacitance between a sphere and an infinite plane is written in terms of a series [20]:

$$C_{\text{sp}} = 4\pi\epsilon_0 R \sinh(\alpha) \sum_{n=1}^{+\infty} \frac{1}{\sinh(n\alpha)} \quad (1)$$

with  $\cosh(\alpha) = 1 + d/R$ ,  $R$  is the sphere radius, and  $d$  the separation distance. In the limit of small separations,  $d/R \ll 1$ , an approximate expression for the capacitance can be obtained [20]:

$$C_{\text{sp}} \approx 2\pi\epsilon_0 R \left( \ln \frac{R}{d} + \ln 2 + \frac{23}{20} + \frac{\theta}{63} \right) \quad (2)$$

where  $0 \leq \theta \leq 1$ . By neglecting the distance-independent terms one obtains an expression often appearing in relationship to the so-called Proximity Force Approximation (PFA) [21, 22] in electrostatics. The formulas above both assume an infinite plane and a whole sphere. In real experiments involving microresonators the size of the plane is not necessarily large enough to be considered infinite and thus edge effects could be present. In some measurements [17] the sphere is located close to one end of the squared plane, to increase the torque exerted on the underlying microresonator. Also, in other measurements a lens, schematized as a truncated sphere was used in lieu of a whole sphere [14, 23]. Fig. 3 shows the numerical results for configurations taking into account these deviations from the idealized case, as well as the curves expected from the exact (1) and the approximate (2) expressions.

For the whole sphere, it is worth remarking that neither the exact nor the approximate expression can give an accurate value for the capacitance between a sphere and a finite plane, even at small distance. We have checked that the idealized case of a sphere and an infinite plane is approached by considering square plates of progressively larger size. The capacitance in the realistic case still preserves a logarithmic dependence at small distance, with the slopes very close to each other. For the truncated sphere, the capacitance is significantly smaller than both the exact and the approximate expressions, which is expected considering that there is less conducting surface available in this case. Moreover, much smaller distance is required for the capacitance to be approximated by a logarithmic dependence with a slope comparable to the one of the whole sphere case. The truncation aspect ratio has been chosen in close analogy on the case of the lenses used in the sphere-plane experiment reported in [23], and it should also be similar to the one used in the first modern Casimir force experiment in the sphere-plane configuration [14].

### 4. CYLINDER-PLANE GEOMETRY

For the cylinder-plane geometry, the expression for the capacitance between a cylinder and an infinite plane is

$$C_{\text{cp}} = \frac{2\pi\epsilon_0 L}{\cosh^{-1}(1 + d/R)} \quad (3)$$

where  $L$  and  $R$  are the length and radius of the cylinder, and  $d$  the distance. In the limit of small separations,  $d/R \ll 1$ , an approximate expression for the capacitance can be obtained by expanding the inverse hyperbolic cosine function with Puiseux series [24]:

$$C_{\text{cp}} \approx \frac{\sqrt{2R}\pi\epsilon_0 L}{d^{0.5}}. \quad (4)$$

Beside the finite size of the plane, the finite length of the cylinder may also be a source of deviation from ideality. Therefore we have considered two cases, differing in the

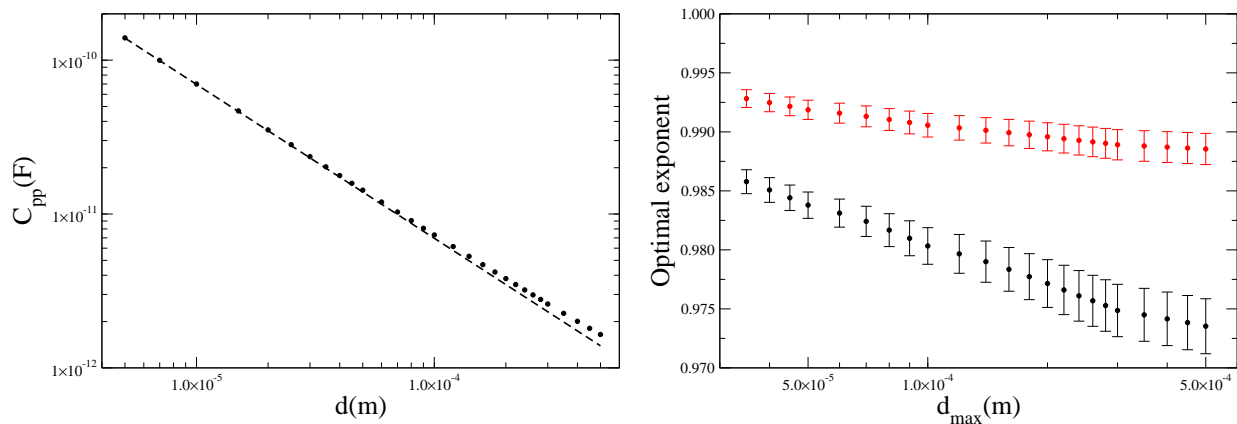


FIG. 2: (Left) Capacitance *vs.* distance for two parallel square plates. Dots indicate the results of the numerical simulation, while the dashed line is the capacitance expected using the formula  $C_{pp} = \epsilon_0 A/d$ . The length of the square plates  $L$  was chosen to be 8.86 mm. (Right) Optimal exponent  $\epsilon_c$  coming from the best fit of a set of numerical data with  $C_{pp} = \epsilon_0 A/(d - d_0)^{\epsilon_c}$  *vs.* the distance of the farthest data point used in the fitting. Red dots are obtained by fixing  $d_0=0$ , corresponding to an *a priori* knowledge of the absolute distance, while the black squares are obtained if  $d_0$  is considered as a fitting parameter, as usually done when analyzing real experimental data with no *a priori* independent knowledge of the absolute distance between the two surfaces. Considering the size of the square plates used in the experiment reported in [13] of 1.1 mm, all separation distances in that case are obtained by scaling down the horizontal axis by a factor  $\simeq 65$ .

length of the cylinder chosen as smaller or larger than the side length of the plane, and the analysis has been repeated for truncated cylinders. The capacitance per unit length  $C_{cp}/L_{eff}$  *vs.* distance for different configurations are shown in Fig. 4. In this figure  $L_{eff}$  is defined as the minimum between the length of the cylinder and the length of the plane along the cylinder axis, *i.e.* defining the *overlapping* area between the cylinder and the plane. As can be seen in Fig. 4, truncated, wider cylinders deviate less from the exact expression in comparison to whole, narrower cylinders. However, longer width means harder parallelization and consequently worse achievable minimum distance. From Fig. 4, a narrow truncated cylinder seems to be a good compromise, which is the configuration used in realistic experiments.

## 5. IMPLICATIONS FOR THE ELECTROSTATIC CALIBRATIONS IN CASIMIR FORCE EXPERIMENTS

The discussion above shows that when the sizes of the samples are finite and the edge effects cannot be ignored, the capacitance will not scale with distance through the exponent expected from the ideal formula. If the exponent is incorrectly forced to the value from the ideal formula in the data fitting procedure, systematic errors will be propagated to all the fitting parameters. In fact, the optimal exponent is not a constant and depends on distance as evident in the plane-plane configuration shown in Fig. 2, therefore assuming a constant optimal exponent over the entire range of explored distances will generate systematic errors in the electrostatic calibrations.

Let us consider the cylinder-plane geometry as an example. As already mentioned, in a real experiment it is hard to determine directly the absolute separation distance, and only data fitting allows to obtain the separation if considered as a fitting parameter (see also the detailed discussion in [25] on the same definition of distance between two macroscopic bodies). In the ideal case, by fitting the capacitance data with a relationship like

$$C_{cp} = C_0 + K_c/(d - d_0)^{\epsilon_c} \quad (5)$$

with the exponent  $\epsilon_c = 0.5$  and  $C_0$ ,  $K_c$  and  $d_0$  as fitting parameters, the absolute distance can be obtained as  $d_{abs} = d - d_0$ . Here  $C_0$  represents a constant fitting parameter due to background, parasitic, distance-independent capacitance added to the cylinder-plane capacitance, obtainable in the limit of very large gap separation. In the case of our numerical simulation data, we can fix  $C_0 = 0$ . If the correct fitting equation is used, the value of  $d_0$  obtained should agree within the fitting errors with the expected null value. By fitting with Eq. (5) the simulation data of the narrow truncated cylinder up to distance 10  $\mu\text{m}$ , the maximum distance at which electrostatic calibrations are usually carried out,  $d_0 = -18 \pm 3$  nm is obtained with the exponent  $\epsilon_c$  is fixed at 0.5, while we obtain  $d_0 = 12 \pm 1$  nm if  $\epsilon_c$  is left as a free parameter, with an optimal value of  $0.4849 \pm 0.0005$ . In both cases, the value of  $d_0$  from the fitting is different from zero by several standard deviations. The smallest distance in the data is 400 nm, -18 nm and 12 nm represent errors with respect to the smallest gap separation of 4.5 % and 3.0%, respectively. Similar analysis can be repeated for the parallel square plates, and the whole and truncated sphere

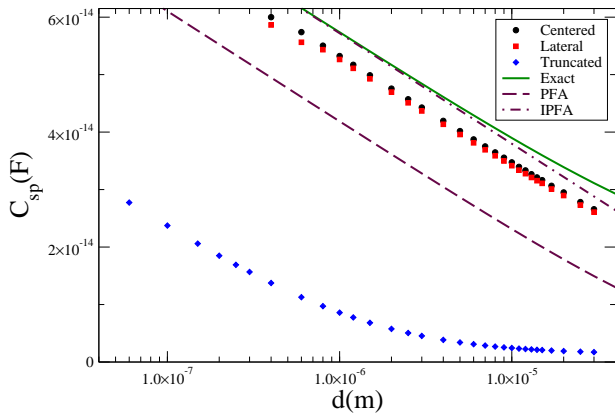


FIG. 3: Capacitance dependence on distance in the sphere-plane configurations. The case of a whole sphere located above the center of a square plate (black dots) and on the edge of the plate (red squares) are shown, as well as the case of a truncated sphere (blue diamonds). The radius of the sphere is chosen to be 0.15 mm and the length of the square plate 0.5 mm. The continuous line corresponds to the exact expression as in (1), and the dashed dot line corresponds to the approximate expression as in (2), named Improved PFA (IPFA), while the dashed line is the capacitance expected from the PFA method.

configuration by fitting the data respectively with

$$\begin{aligned} C_{pp} &= C_0 + K_c/(d - d_0)^{\epsilon_c}, \\ C_{sp} &= C_0 + K_c \ln(d - d_0). \end{aligned} \quad (6)$$

The results are shown in Table I, where the values of  $d_0$  are all significantly different from the expected null value. To show that this is not a fitting artifact, the same fitting procedures have been repeated with simulation data at much smaller distance where the edge effects can be safely ignored. In this check the values of  $d_0$  agree with the expected value of zero within the associated error from the fitting procedure. Therefore it is evident that the presence of edge effects may result in significant systematic errors in the best fit, affecting the accuracy of crucial parameters such as the absolute distance.

With regard to Casimir experiments, other crucial parameters of the experiment beside the absolute distance between the two surfaces are determined through the electrostatic calibrations, for instance the effective mass  $m_{\text{eff}}$  of the resonator or, equivalently, its stiffness. The calibrations are usually done at relatively large distance to ensure that the Casimir force can be neglected. However, in this regime the edge effects become more significant leading to systematic errors in the fitting procedures as shown above. However, in most Casimir experiments what is measured in the calibrations, rather than the capacitance, is the electrostatic force between the two surfaces or, if a resonator is used for dynamical measurements, its square frequency shift [26].

The relationship between these two observables and

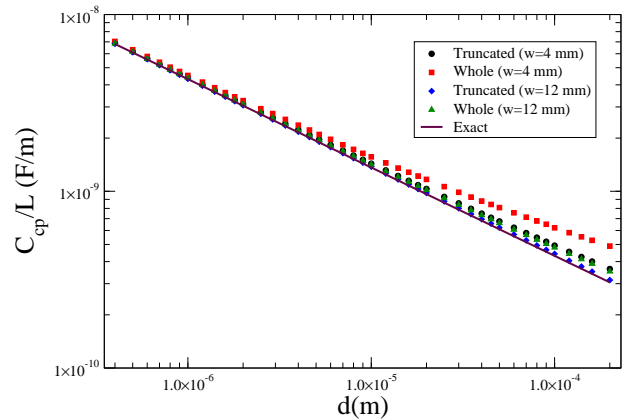


FIG. 4: Simulations in finite-size cylinder-plane configurations. Capacitance per unit of effective length *vs.* distance for a truncated cylinder (black dots) and a whole cylinder (red squares) of width 4 mm in front of a square plane of size 10 mm  $\times$  28 mm, and similar plots for truncated (blue diamonds) and whole (green triangles) cylinders of width 12 mm. The radius of the cylinder is chosen to be 12 mm. The continuous line corresponds to the exact expression as in (3), and the approximate expression (4) coincides with the exact expression in this distance range, confirming that the PFA holds to a high degree of accuracy up to the largest explored distances.

the capacitance is in general given by

$$F_{\text{el}} = -\frac{\partial E_{\text{el}}(d)}{\partial d} = -\frac{1}{2} \frac{\partial C(d)}{\partial d} V^2 \quad (7)$$

$$\Delta \nu_{\text{el}}^2 = -\frac{1}{4\pi^2 m_{\text{eff}}} \frac{\partial F(d)}{\partial d} = \frac{1}{8\pi^2 m_{\text{eff}}} \frac{\partial^2 C(d)}{\partial d^2} V^2. \quad (8)$$

Then the absolute value of the capacitance in itself is irrelevant for force or square frequency shift measurements and, due to the first and second derivatives, the distance dependence of the force or frequency shift signal may end up being less sensitive to the edge effects.

To check the influence of the edge effects on force measurements, numerical differentiation has been carried out, using the Lagrange three-point formula [27], on the simulation capacitance data. The numerical differentiation method works better when the data points are equally spaced, therefore in the case of the sphere-plane configuration the numerical differentiation is performed in the semilogarithmic domain, while for plane-plane and cylinder-plane configurations in the logarithmic domain. Then we fit the force *vs.* distance data with the corresponding equations for each geometry, obtaining the results shown in Table II. It seems that in terms of the optimal exponent, the edge effects are less significant when the force data are considered, apart from the case of the truncated sphere. More specifically, the results for the truncated sphere can be understood as if it behaves like a sphere only at small distance, instead resembles a plane

	Parallel plates	Sphere I	Sphere II	Cylinder
$d_0(\text{nm})$	$-90 \pm 20$	$13 \pm 3$	$144 \pm 13$	$-18 \pm 3$
$d_0/d_{\min}$	1.8%	6.5%	72%	4.5%
$d'_0(\text{nm})$	$140 \pm 20$	N/A	N/A	$12 \pm 1$
$d'_0/d_{\min}$	2.8%	N/A	N/A	3.0%
$\epsilon_c$	$0.977 \pm 0.002$	N/A	N/A	$0.4849 \pm 0.0005$

TABLE I: Parameters of the best fit obtained for the capacitance data in the case of the four configurations considered in the text with Sphere I being whole sphere and Sphere II truncated sphere. For parallel plates and cylinder-plane configurations, the top two rows are the parameters obtained when the exponent  $\epsilon_c$  is fixed at 0.5 and 1, and the bottom three rows when  $\epsilon_c$  is left as a free parameter. For the sphere-plane configuration, due to the logarithmic dependence of the capacitance scales with distance, no exponent can be introduced.

when considered at large distance from the plane. This result is at variance with respect to the behavior actually observed in [5], since a square frequency shift power law dependence on distance with an exponent less than 2 (therefore corresponding to a force exponent  $\epsilon_f < 1$ ) has been observed uniformly over the entire range of explored distances. Therefore the origin of the anomaly observed in [5] cannot be ascribed to edge effects. Analogous considerations can be repeated for the first derivative of the force whenever square frequency shifts are measured. The influence of the edge effects on the values of fitting parameters  $d_0$  and  $K_f$  in force measurement is also less significant at relatively small distance in the case of parallel plates, truncated cylinder and whole sphere, while in the case of the truncated sphere the error is much more significant. However, although the edge effects are not as strong in force measurement as in capacitance measurement, related systematic errors are still present, especially at large distance. Therefore the edge effects need to be considered and carefully examined if high precision measurements are required, and the robustness of the fitting procedure with respect to the choice of the distance range becomes crucial for the parameters, in particular  $K_f$  and  $d_0$ .

## 6. CONCLUSION

We have analyzed the effect of finite size in the predictions for the electrostatic calibrations of geometries of interest for measuring the Casimir force. One relevant consideration arising, or better quantitatively confirmed, from this numerical study is that there is a trade-off in the choice of the distance range to perform electrostatic calibrations. If this range is including too close distances, roughness corrections and the presence of the attractive Casimir force may result in systematic effects, while if large distance data are also considered one must include

edge effects in the theoretical modelization of the experimental setup for a targeted level of accuracy of the electrostatic calibrations. If geometrical configurations manifestly differing from the idealized cases are also considered, such as a small portion of a sphere or a truncated cylinder, the deviations in the capacitance are even more pronounced and a full numerical evaluation of the electrostatics is necessary even at relatively moderate levels of desired accuracy. We have also shown that force (gradient force) measurements, based on the first (second) derivative with respect to distance of the capacitance, are in general more robust than absolute capacitance measurement in itself with respect to the geometrical deviations from ideality, confirming from another perspective a point recently discussed in [28]. Finally, we want to point out that detecting edge effects provides also a simple and reliable method to assess the precision of the electrostatic calibrations, for instance determining the minimum separation gap above which deviations attributable to finite edges are effectively observed.

## ACKNOWLEDGMENTS

We acknowledge useful discussions with D. A. R. Dalvit.

## REFERENCES

- 
- [1] H.B.G. Casimir, Proc. K. Ned. Akad. Wet. B 51 (1948) 793.
  - [2] E. Fischbach and C.L. Talmadge, The Search for Non-Newtonian Gravity, AIP/Springer-Verlag, New York, 1999.
  - [3] A. Lambrecht and S. Reynaud, Eur. Phys. J. D 8 (2000) 309.
  - [4] R. Onofrio, New J. Phys. 8 (2006) 237.
  - [5] W.J. Kim, M. Brown-Hayes, D.A.R. Dalvit, J.H. Brownell, and R. Onofrio, Phys. Rev. A 78 (2008) 020101(R); J. Phys. Conf. Ser. 161 (2009) 012004.
  - [6] W.J. Kim, A.O. Sushkov, D.A.R. Dalvit, and S.K. Lamoreaux, Phys. Rev. Lett. 103 (2009) 060401; S. de Man, K. Heeck, and D. Iannuzzi, Phys. Rev. A 79 (2009) 024102; R.S. Decca, E. Fischbach, G.L. Klimchitskaya, D.E. Krause, D. Lopez, U. Mohideen, and V.M. Mostepanenko, Phys. Rev. A 79 (2009) 026101; W.J. Kim, D.A.R. Dalvit, M. Brown-Hayes, J.H. Brownell, and R. Onofrio, Phys. Rev. A 79 (2009) 026102.
  - [7] C.C. Speake, and C. Trenkel, Phys. Rev. Lett. 90 (2003) 160403.
  - [8] W. J. Kim, A.O. Sushkov, D.A.R. Dalvit, and S.K. Lamoreaux, Phys. Rev. A 81 (2010) 022505.
  - [9] H. Gies and K. Klingmüller, Phys. Rev. Lett. 97 (2006) 220405.

Geometry	Fitting range ( $\mu\text{m}$ )	$K_f(\text{Nm}^{\epsilon_f}\text{V}^2)$	$\epsilon_f$	$d_0(\text{nm})$	$d_0/d_{\min}$
Parallel plates	7 – 50	$(3.59 \pm 0.03) \times 10^{-16}$	$1.9971 \pm 0.0007$	$10.5 \pm 2.9$	0.15%
	50 – 450	$(4.4 \pm 1.0) \times 10^{-16}$	$1.973 \pm 0.025$	$800 \pm 760$	1.6%
Whole sphere	0.2 – 3	$(6.1 \pm 6.8) \times 10^{-15}$	$0.97 \pm 0.08$	$2 \pm 19$	1.0%
	3 – 25	$(1.4 \pm 2.0) \times 10^{-15}$	$1.10 \pm 0.12$	$-430 \pm 410$	14.3%
Truncated sphere	0.2 – 3	$(4.3 \pm 2.8) \times 10^{-17}$	$1.30 \pm 0.04$	$-35 \pm 10$	17.5%
	3 – 25	$(1.4 \pm 0.6) \times 10^{-21}$	$1.92 \pm 0.04$	$-480 \pm 80$	16.0%
Truncated cylinder	0.5 – 10	$(36.4 \pm 2.2) \times 10^{-16}$	$1.513 \pm 0.005$	$-5.8 \pm 2.0$	1.2%
	10 – 160	$(29.2 \pm 6.2) \times 10^{-16}$	$1.538 \pm 0.020$	$-370 \pm 180$	3.7%

TABLE II: Parameters of the best fit obtained considering an electrostatic-like force obtained leaving the power exponent for the distance dependence, as a free parameter in the cases of the four configurations considered in the text. The parameter  $K_f$  is the electrostatic coefficient,  $\epsilon_f$  the optimal exponent for the force measurement, and  $d_0$  an offset in distance, such that the electrostatic force can be expressed as  $F_{el} = F_0 + K_f V^2 / (d - d_0)^{\epsilon_f}$ .

- [10] A. Weber and H. Gies, Phys. Rev. D 80 (2009) 085007.
- [11] T. Ederth, Phys. Rev. A 62 (2000) 062104.
- [12] M.J. Sparnaay, Physica 24 (1958) 751.
- [13] G. Bressi, G. Carugno, R. Onofrio, and G. Ruoso, Phys. Rev. Lett. 88 (2002) 041804.
- [14] S.K. Lamoreaux, Phys. Rev. Lett. 78 (1997) 5.
- [15] U. Mohideen and A. Roy, Phys. Rev. Lett. 81 (1998) 4549; B.W. Harris, F. Chen, and U. Mohideen, Phys. Rev. A 62 (2000) 052109.
- [16] H. B. Chan, V.A. Aksyuk, R.N. Kleiman, D.J. Bishop, and F. Capasso, Phys. Rev. Lett. 87 (2001) 211801; D. Iannuzzi, I. Gelfand, M. Lisanti, and F. Capasso, Proc.Nat. Ac. Sci. USA 101 (2004) 4019.
- [17] R.S. Decca, D. Lopez, E. Fischbach, and D.E. Krause, Phys. Rev. Lett. 91 (2003) 050402; R.S. Decca *et al.*, Phys. Rev. Lett. 94 (2005) 240401.
- [18] D. A. R. Dalvit, F. C. Lombardo, F. D. Mazzitelli, and R. Onofrio, Europhys. Lett. 67 (2004) 517; M. Brown-Hayes, D.A.R. Dalvit, F.D. Mazzitelli, W.J. Kim, and R. Onofrio, Phys. Rev. A 72 (2005) 052102; M. Brown-Hayes, J.H. Brownell, D.A.R. Dalvit, W.-J. Kim, A. Lambrecht, F.C. Lombardo, F.D. Mazzitelli, S.M. Middleman, V.V. Nesvizhevsky, and R. Onofrio, J. Phys. A 39 (2006) 6195.
- [19] H. J. Wintle and S. Kurylowicz, IEEE Trans. Instr. Meas. vol. IM-34 (1985) 41.
- [20] L. Boyer, F. Houze, A. Tonck, J.L. Loubet, and J.M. Georges, J. Phys. D: Appl. Phys. 27 (1994) 1504.
- [21] B. V. Derjaguin and I. I. Abrikosova, Sov. Phys. JETP 3 (1957) 819.
- [22] J. Blocki, J. Randrup, W. I. Swiatecki, and F. Tsang, Ann. Phys. 105 (1977) 427.
- [23] W. J. Kim, M. Brown-Hayes, D. A. R. Dalvit, J. H. Brownell, and R. Onofrio, Phys. Rev. A 78 (2008) 020101(R).
- [24] V. A. Puisseux, J. Math. Pures Appl. 15 (1850) 365; 16 (1851) 228; N. J. A. Sloane, Sequence A091019 in "The On-Line Encyclopedia of Integer Sequences".
- [25] P. J. van Zwol, V. B. Svetovoy, and G. Palasantzas, Phys. Rev. B 80 (2009) 235401.
- [26] G. Bressi, G. Carugno, A. Galvani, R. Onofrio, and G. Ruoso, Class. Quant. Grav. 17 (2000) 2365; G. Bressi, G. Carugno, A. Galvani, R. Onofrio, G. Ruoso, and F. Veronese, Class. Quant. Grav. 18 (2001) 3943.
- [27] M. Combrinck, Comput. Geosci. 35 (2009) 1563.
- [28] R. S. Decca, E. Fischbach, G. L. Klimchitskaya, D. E. Krause, D. Lopez, U. Mohideen, and V. M. Mostepanenko, arXiv:0904.4720 (29 April 2009).